



## Convective Flow of Blood through a Constricted Cylinder and the Effect of Cholesterol Growth Rate on the Motion in the Presence of a Magnetic Field

K. W. Bunonyo<sup>a,\*</sup>, E. Amos<sup>b</sup>

<sup>a</sup>Department of Mathematics and Statistics, Federal University Otuoke (FUO), Nigeria

<sup>b</sup>Department of Mathematics, Rivers State University, Nigeria

---

### Abstract

An inflammatory disease resulting in the pathological constriction of the intima and media of the arterial system, such as the aorta, causes symptoms like stroke, heart attack, or angina; This research investigates the convective flow of blood through a constricted cylinder and the effect of cholesterol growth rate on the motion in the presence of a magnetic field by transforming the problem into a system of time-dependent partial differential equations. The governing partial differential equations (PDEs) were transformed into dimensionless ordinary differential equations (ODEs) and solved using the Laplace method. After obtaining the analytical solution, Wolfram Mathematica was used to perform the numerical computation where the various physical parameters such as Soret number, radiation number, solutal Grashof number, Schmidt number, and Prandtl number were varied to their impact studied. The study discovered that increasing the Soret number causes an increase in blood velocity, whereas decreasing the Solutal Grashof number decreases blood velocity. Furthermore, an increase in radiation parameter increases the blood velocity, but a Soret number increase results in a decrease in the concentration of cholesterol in the fluid, a Schmidt number, and oscillatory frequency increase, causing the temperature to decrease. This research is useful for clinicians and mathematical modellers who are trying to understand the flow of cholesterol saturated fluid in the human vascular system and how best to proffer analytical and numerical solutions in synergy with laboratory investigation.

DOI:10.46481/asr.2022.1.3.56

*Keywords:* Blood, Convection, Cholesterol, Growth, Motion, Magnetic field, Cylinder, LDL

### Article History :

Received: 31 August 2022

Received in revised form: 12 October 2022

Accepted for publication: 14 October 2022

Published: 29 December 2022

© 2022 The Author(s). Published by the Nigerian Society of Physical Sciences under the terms of the Creative Commons Attribution 4.0 International license. Further distribution of this work must maintain attribution to the author(s) and the published article's title, journal citation, and DOI.

Communicated by: Tolulope Latunde

---

\*Corresponding author tel. no: +234 8034367252

Email address: wilcoxbk@fuotuo.ke.edu.ng (K. W. Bunonyo)

## 1. Introduction

Atherosclerosis is an inflammatory disease resulting in the pathological constriction of the intima and media of the arterial system, such as the aorta, causing symptoms like stroke, heart attack, or angina. Atherosclerosis is the leading cause of death in western societies. It is characterized by an accumulation of excessive cholesterol and inflammatory cells and lipids in the intima and media, leading to their thickening and hence to a constriction of the arterial lumen. It is now well accepted that a significant first step in the initiation of the early atherosclerotic process is a dysfunction of the endothelium, allowing the penetration of low-density lipoproteins (LDL) through the monolayer of endothelial cells into the vessel wall. Therefore, the role of the endothelium is crucial since it acts as a transportation barrier between the lumen and the intima. According to Bunonyo *et al.* [1], LDL in the vessel wall is prone to oxidative modifications, initiating the inflammatory processes. Below is some research that talks about atherosclerosis and constriction. They are: Ambrosi & Mollica [2] studied tumor growth within the framework of continuum mechanics, considering a tumor as a specific case of growing soft tissue. They used the notion of multiple natural configurations in which they introduced a mechanical description that splits volumetric growth and mechanical response into two separate contributions. Growth is described as an increase in the mass of the particles of the body and not as an increase in their number. The finding that tumor growth strongly depends upon the availability of nutrients and the presence of chemical signals, such as growth factors, their diffusion through the growing material is introduced in the description. According to Balzani and Schmidt [3], there are several damage equations that analyze the properties of atdamage initialization. The study is important for soft tissues since two different loading regimes have to be clearly distinguished: the physiological domain where no damage evolution should be considered and the supra-physiological domain wheredamage evolves. Barrenechea & Valentin [4] used an unusual stabilized finite element that is presented and analyzed to investigate a generalized Stokes problem with a dominating zeroth order term. The method consists of subtracting a mesh-dependent term from the formulation without compromising consistency. The design of this mesh-dependent term, as well as the stabilization parameter involved, is suggested by bubble condensation. Stability is proven for any combination of velocity and pressure spaces, under the hypothesis of continuity for the pressure space. Bazilevs *et al.* [5] elucidated left ventricular assist devices (LVADs) as continuous flow pumps that are employed in patients with severe heart failure. Although their emergence has significantly improved therapeutic options for patients with heart failure, detailed studies of the impact of LVADs on hemodynamics are notably lacking. They initiated a computational study of the Jarvik 2000 LVAD model employing isogeometric fluid–structure interaction analysis. Brown *et al.* [6] investigated the major causes of morbidity and mortality worldwide and said that a thorough understanding of the underlying pathophysiological mechanisms is crucial for the development of new therapeutic strategies. Although atherosclerosis is a systemic inflammatory disease, coronary atherosclerotic plaques are not uniformly distributed in the vascular tree. Calvez *et al.* [7] used a mathematical model to describe the early formation of atherosclerotic lesions. According to the investigator, the early stage of atherosclerosis is an inflammatory process that starts with the penetration of low-density lipoproteins into the intima and with their oxidation. This phenomenon is closely linked to the local blood flow dynamics. Chalmers *et al.* [8] investigated the bifurcation and dynamics in a mathematical model of early atherosclerosis. The study involved the interactions between modified low density lipoprotein (LDL) and monocytes or macrophages. This model suggests that there is an initial inflammatory phase associated with atherosclerotic lesion development and a longer, quasi-static process of plaque development inside the arterial wall that follows the initial transient. Chen and Lu [9] elucidated the pulsatile flow of non-Newtonian fluid in a bifurcation model with a non-planar daughter branch numerically by using the Carreau–Yasuda model to take into account the shear thinning behavior of the analogue blood fluid. The objective of this study is to deal with the influence of the non-Newtonian property of fluid and of out-of-plane curvature in the non-planar daughter vessel on wall shear stress (WSS), oscillatory shear index (OSI), and flow phenomena during the pulse cycle. The calculated results for the pulsatile flow support the view that the non-planarity of blood vessels and the non-Newtonian properties of blood are an important factor in hemodynamics and may play a significant role in vascular biology and pathophysiology. According to Cheng *et al.* [10], wall shear stress (WSS), the frictional force between blood and endothelium, is an important determinant of vascular function. It is generally assumed that WSS remains constant at a reference value of  $15 \text{ dyn/cm}^2$ . In a study of small rodents, they realized that this assumption could not be valid. Cho and Kensey [11] studied the effects of the non-Newtonian viscosity of blood on the flow in a coronary arterial cast of a man were studied numerically using a finite element method. They investigated the various constitutive models to model the non-Newtonian viscosity of blood and their model constants were summarized. A method to incorporate the non-

Newtonian viscosity of blood was introduced so that the viscosity could be calculated locally. Cilla [12] investigated atherosclerosis as a vascular disease caused by inflammation of the arterial wall, which results in the accumulation of low-density lipoprotein (LDL) cholesterol, monocytes, macrophages, and fat-laden foam cells at the site of the inflammation. This process is commonly referred to as plaque formation. The evolution of atherosclerosis disease, and in particular the influence of wall shear stress on the growth of atherosclerotic plaques, is still a poorly understood phenomenon. Codina [13] presented a stabilized finite element method to solve the Navier–Stokes equations based on the decomposition of the unknowns into resolvable and subgrid scales. The first is a method to estimate the behavior of the stabilization parameters based on a Fourier analysis of the problem for the subscales. Secondly, the way to deal with transient problems discretized using a finite difference scheme is discussed. Finally, the treatment of the nonlinear term is analyzed. Crosetto *et al.* [14] used the numerical tools to simulate blood flow in the cardiovascular system that are constantly developing due to the great clinical interest and to scientific advances in mathematical models and computational power. De Wilde *et al.* [15] studied the low and oscillatory wall shear stresses near the aortic bifurcation linked to the onset of atherosclerosis. The studies were based on simulations of boundary conditions measured under anesthesia. Moradicheghamahi *et al.* [16] investigated the risk factor at the carotid bifurcation as a result of the changes in the flow of blood and phenomena such as flow separation, rotational flow, and the effects of the shear stress induced by the walls, increasing the risk of injury. The study numerically simulates the pulsatile flow of the blood in a patient-specific elastic carotid artery with physiological pulses and non-Newtonian and turbulent models. Hanvey and Bunonyo [17] carried out an investigation into the influence of treatment parameters on the flow of blood in a stenosed artery in the presence of a magnetic field with heat transfer. They solved the momentum equation governing by scaling it to a dimensionless structure with the aid of some dimensionless parameters. The equations have been analytically solved using the modified Bessel equation and by the method of undetermined coefficients in order to obtain the temperature profile and velocity profile of the blood flow. The model analysis and results are presented graphically with the help of the software Mathematica. Kubugha and Amos [18] used a mathematical model to investigate LDL-C and blood flow through an inclined channel with heat in the presence of a magnetic field. In their research, mathematical models were formulated to represent LDL-C and blood flow and energy transfer as a coupled system of partial differential equations (PDEs). The PDEs were scaled using the dimensionless quantities to dimensionless partial differential equations. They further reduced the equations to ordinary differential equations (ODEs) using the perturbation method involving the oscillatory term. Thereafter, governing equations are solved directly using the method of undetermined coefficient. The above literature failed to address the convective flow of blood through a constricted cylinder and the effect of cholesterol growth rate on the motion in the presence of a magnetic field. The goal of this research is to formulate coupled mathematical models that represent the problem, solve the transformed equations using the Laplace method, and perform numerical simulation using Mathematica, to investigate the impact of the thermo-physical parameters on the flow profiles.

## 2. Mathematical Formulation

Consider a convective flow of blood, an electrically conducting, and incompressible viscous, and non-Newtonian fluid, flowing through an atherosclerotic artery presumed to be a cylindrical channel with a velocity  $w^*(r^*, x^*)$ , where  $r^*$  and  $x^*$  indicating the direction of the flow, and the channel is filled with cholesterol-laden fatty substances which grows exponentially. The tangential velocity is assumed to be zero and the pressure is generated towards the axial direction. We assume the application of perpendicular external magnetic field. Following Bunonyo and Ebiwareme [19], we present mathematical representation of atherosclerotic geometry and the governing equations as follows:

### 2.1. The geometry of constriction

$$R = \begin{cases} R_0 - \frac{\delta^*}{2} \left(1 + \cos \frac{2\pi x^*}{\lambda^*}\right) & \text{at } d_0 \leq x^* \leq \lambda^* \\ R_0 & \text{at } 0 \leq x^* \leq d_0 \end{cases} \quad (1)$$

where

$$x^* = \left(d_0 + \frac{\lambda^*}{2}\right) \quad (2)$$

2.2. Momentum Equation

$$\rho_b \frac{\partial w^*}{\partial t^*} = -\frac{\partial P^*}{\partial x^*} + \mu_b \left( \frac{\partial^2 w^*}{\partial r^{*2}} + \frac{1}{r^*} \frac{\partial w^*}{\partial r^*} \right) - \frac{\mu_b \varphi}{k^*} w^* - \sigma B_0^2 w^* + \rho_b g \beta_C (C^* - C_\infty) \tag{3}$$

2.3. Heat Equation

$$\rho_b c_b \frac{\partial T^*}{\partial t^*} = k_{Tb} \left( \frac{\partial^2 T^*}{\partial r^{*2}} + \frac{1}{r^*} \frac{\partial T^*}{\partial r^*} \right) - Q_0 (T^* - T_\infty) \tag{4}$$

2.4. Concentration Equation

$$\frac{\partial C^*}{\partial t^*} = D_m \left( \frac{\partial^2 C^*}{\partial r^{*2}} + \frac{1}{r^*} \frac{\partial C^*}{\partial r^*} \right) + \frac{D_T k_T}{T_m} \left( \frac{\partial^2 T^*}{\partial r^{*2}} + \frac{1}{r^*} \frac{\partial T^*}{\partial r^*} \right) \tag{5}$$

The corresponding initial and boundary conditions are

$$\left. \begin{aligned} w^* = 0, T^* = T_w, C^* = C_w \text{ at } r^* = R \\ w^* \neq 0, T^* \neq T_\infty, C^* \neq C_\infty \text{ at } r^* = 0 \end{aligned} \right\} \tag{6}$$

2.5. Dimensionless Parameters

$$\left. \begin{aligned} x = \frac{x^*}{\lambda^*}, r = \frac{r^*}{R_0}, t = \frac{t^* v_b}{R_0^2}, w = \frac{w^* R_0}{v_b}, \theta = \frac{T^* - T_\infty}{T_w - T_\infty}, S_r = \frac{D_T k_{Tb}}{v_b T_m} \left( \frac{T_w - T_\infty}{C_w - C_\infty} \right), \\ Rd_1 = \frac{Q_0 R_0^2}{\mu_b c_b}, Gc = \frac{g \beta_C (C_w - C_\infty) R_0^3}{v_b^2}, M = B_0 R_0 \sqrt{\frac{\sigma}{\mu_b}}, \frac{1}{k} = \frac{\varphi R_0^2}{k^*}, r = h \\ Sc = \frac{v_b}{D_m}, \delta^* = \frac{\delta R_0 e^{at}}{R_T}, Pr = \frac{\mu_b c_b}{k_{Tb}}, P = \frac{R_0^3 P^*}{\lambda^* \mu_b v_b}, \phi = \frac{C^* - C_\infty}{C_w - C_\infty}, \frac{\delta}{R_0} \ll 1 \end{aligned} \right\} \tag{7}$$

Reducing the governing equations (1)-(6) using equation (7), we have the following:

$$\frac{R}{R_0} = \begin{cases} 1 - \frac{\delta}{2R_T} e^{at} (1 + \cos 2\pi x) & \text{at } d_0 \leq x^* \leq \lambda^* \\ 1 & \text{at } 0 \leq x^* \leq d_0 \end{cases} \tag{8}$$

where

$$x = \frac{1}{\lambda} \left( d_0 + \frac{\lambda}{2} \right) \tag{9}$$

$$\frac{\partial w}{\partial t} = -\frac{\partial P}{\partial x} + \left( \frac{\partial^2 w}{\partial r^2} + \frac{1}{r} \frac{\partial w}{\partial r} \right) - \frac{1}{k} w - M^2 w + Gr\theta + Gc\phi \tag{10}$$

$$Pr \frac{\partial \theta}{\partial t} = \left( \frac{\partial^2 \theta}{\partial r^2} + \frac{1}{r} \frac{\partial \theta}{\partial r} \right) - Rd_1 Pr \theta \tag{11}$$

$$Sc \frac{\partial \phi}{\partial t} = \left( \frac{\partial^2 \phi}{\partial r^2} + \frac{1}{r} \frac{\partial \phi}{\partial r} \right) + S_r Sc \left( \frac{\partial^2 \theta}{\partial r^2} + \frac{1}{r} \frac{\partial \theta}{\partial r} \right) \tag{12}$$

The corresponding boundary conditions are

$$\left. \begin{aligned} w \neq 0, \theta \neq 0, \phi \neq 0 \text{ at } r = 0 \\ w = 0, \theta = 1, \phi = 1 \text{ at } r = \frac{R}{R_0} \end{aligned} \right\} \tag{13}$$

### 2.6. Reduction of the Governing Equations to ODEs

Since the pressure is generated by the ventricular action in the axial direction, the governing equations can be reduced to ODEs by adopting the following:

$$\left. \begin{aligned} w(r, t) &= w_0(r) e^{i\omega t}, \theta(r, t) = \theta_0(r) e^{i\omega t} \\ \phi(r, t) &= \phi_0(r) e^{i\omega t}, -\frac{\partial P}{\partial x} = P_0 e^{i\omega t} \end{aligned} \right\} \tag{14}$$

Following equation (14), the governing equations (10)-(13) are reduced to:

$$\frac{d^2 w_0}{dr^2} + \frac{1}{r} \frac{dw_0}{dr} - \beta_1^2 w_0 = P_0 - Gc\phi_0 \tag{15}$$

$$\frac{d^2 \theta_0}{dr^2} + \frac{1}{r} \frac{d\theta_0}{dr} - \beta_2^2 \theta_0 = 0 \tag{16}$$

$$\frac{d^2 \phi_0}{dr^2} + \frac{1}{r} \frac{d\phi_0}{dr} - \beta_4^2 \phi_0 + S_r S_c \left( \frac{d^2 \theta_0}{dr^2} + \frac{1}{r} \frac{d\theta_0}{dr} \right) = 0 \tag{17}$$

The corresponding boundary conditions are

$$\left. \begin{aligned} w_0 \neq 0, \theta_0 \neq 0, \phi_0 \neq 0 & \quad \text{at } r = 0 \\ w_0 = 0, \theta_0 = e^{-i\omega t}, \phi_0 = e^{-i\omega t} & \quad \text{at } r = \frac{R}{R_0} \end{aligned} \right\} \tag{18}$$

### 3. Method of Solution

We would solve equations (15)-(17), subject to the boundary conditions in equation (18) using the Laplace method. The method can be stated as follows:

$$L\{w_0(r)\} = w_0(s) = \int_0^\infty w_0(r) e^{-rs} dr \tag{19}$$

$$L\{\theta_0(r)\} = \theta_0(s) = \int_0^\infty \theta_0(r) e^{-rs} dr \tag{20}$$

$$L\{\phi_0(r)\} = \phi_0(s) = \int_0^\infty \phi_0(r) e^{-rs} dr \tag{21}$$

To solve equation (16), we would adopt equation (20), which can be applied as follows:

$$L\left\{r \frac{d^2 \theta_0}{dr^2}\right\} + L\left\{\frac{d\theta_0}{dr}\right\} + \beta_{21}^2 L\{r\theta_0\} = 0 \tag{22}$$

where  $\beta_{21} = i\beta_2$

Simplifying equation (22), we have

$$L\left\{r \frac{d^2 \theta_0}{dr^2}\right\} + L\left\{\frac{d\theta_0}{dr}\right\} + \beta_{21}^2 L\{r\theta_0\} = 0 = -\frac{d}{ds} (s^2 \theta_0(s) - s\theta_0(0) - \dot{\theta}_0(0)) + s\theta_0(s) - \theta_0(0) - \beta_{21}^2 \frac{d\theta_0}{ds} \tag{23}$$

Simplifying equation (23), we have

$$\frac{d\theta_0}{ds} + \frac{s}{(s^2 + \beta_{21}^2)} \theta_0(s) = 0 \tag{24}$$

Solving equation (24), we have

$$\theta_0(r) = \left( \frac{e^{-i\omega t}}{I_0(\beta_2 h)} \right) I_0(\beta_2 r) \tag{25}$$

where  $J_0(i\beta_2 r) = I_0(\beta_2 r)$

To obtain the temperature profile of the fluid, we substitute equation (25) into equation (14), we have

$$\theta(r, t) = \left( \left( \frac{e^{-i\omega t}}{I_0(\beta_2 h)} \right) I_0(\beta_2 r) \right) e^{i\omega t} \tag{26}$$

To investigate the impact of temperature effect on the cholesterol concentration, differentiate equation (25) twice and substitute the result into equation (17), which is:

$$\frac{d^2\phi_0}{dr^2} + \frac{1}{r} \frac{d\phi_0}{dr} - \beta_4^2\phi_0 = -\frac{S_r S c e^{-i\omega t}}{I_0(\beta_2 h)} \left( \beta_2^2 + \frac{16\beta_2^4 r^2}{64} + \frac{36\beta_2^6 r^4}{2304} + \dots \right) \tag{27}$$

Solving equation (27), the homogenous solution is:

$$\phi_{0h}(r) = A_0 I_0(\beta_4 r) \tag{28}$$

The particular solution to equation (27) can be stated as:

$$\phi_{0p}(r) = A_1 + A_2 r^2 + A_3 r^4 \tag{29}$$

Solving equation (27), we obtained the solution as:

$$\phi_0(r) = A_0 I_0(\beta_4 r) + A_1 + A_2 r^2 + A_3 r^4 \tag{30}$$

See appendix for all the constant coefficients.

The concentration profile is obtained after substituting equation (30) into equation (14), which is:

$$\phi(r, t) = \left( A_0 I_0(\beta_4 r) + A_1 + A_2 r^2 + A_3 r^4 \right) e^{i\omega t} \tag{31}$$

To investigate the effect of concentration on blood momentum, we shall substitute equation (30) into equation (15), which is

$$\frac{d^2 w_0}{dr^2} + \frac{1}{r} \frac{dw_0}{dr} - \beta_1^2 w_0 = P_0 - A_1 Gc - \left( A_0 Gc I_0(\beta_4 r) + A_2 Gc r^2 + A_3 Gc r^4 \right) \tag{32}$$

Applying equation (19) on the homogenous part of equation (32), this is:

$$L \left\{ r \frac{d^2 w_0}{dr^2} \right\} + L \left\{ \frac{dw_0}{dr} \right\} + \beta_{11}^2 L \{ r w_0 \} = 0 \tag{33}$$

Simplifying equation (33), we have

$$L \left\{ r \frac{d^2 w_0}{dr^2} \right\} + L \left\{ \frac{dw_0}{dr} \right\} + \beta_{11}^2 L \{ r w_0 \} = 0 = -\frac{d}{ds} \left( s^2 w_0(s) - s w_0(0) - \dot{w}_0(0) \right) + s w_0(s) - w_0(0) - \beta_{11}^2 \frac{dw_0}{ds} \tag{34}$$

Simplifying equation (34), we obtained the homogenous solution as:

$$w_{0h}(r) = L^{-1} \left\{ \frac{B_3}{\sqrt{(s^2 + \beta_{11}^2)}} \right\} = B_3 L^{-1} \left\{ \frac{1}{\sqrt{(s^2 + \beta_{11}^2)}} \right\} = B_3 J_0(\beta_{11} r) = B_3 J_0(i\beta_1 r) \tag{35}$$

Whereas the particular solution of equation (32) is as follows:

$$w_{0p}(r) = A_4 + A_6 I_0(\beta_4 r) + A_7 r^2 + A_8 r^4 \tag{36}$$

The solution for equation (32) is as follows:

$$w_0(r) = B_3 I_0(\beta_1 r) + A_4 + A_6 I_0(\beta_4 r) + A_7 r^2 + A_8 r^4 \tag{37}$$

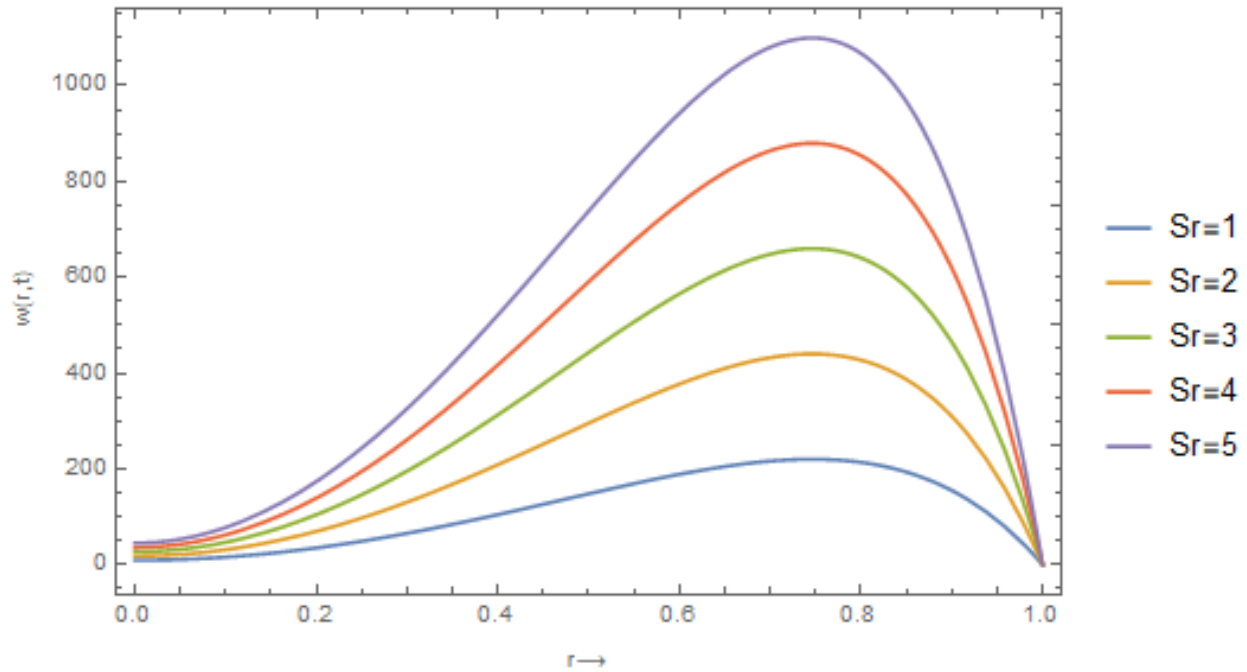


Figure 1. Influence of Soret number on Blood Velocity with other value as  $Gc = 15, Pr = 2.1, Sc = 2, Rd_3 = 2, Rd_1 = 2, \omega = 0.3, k = 0.05, M = 1.5, x = 0.5$

Having simplified the concentration effect on blood velocity, the solution for equation (32) is:

$$w(r, t) = \left( B_3 I_0(\beta_1 r) + A_4 + A_6 I_0(\beta_4 r) + A_7 r^2 + A_8 r^4 \right) e^{i\omega t} \tag{38}$$

The volumetric flow rate can be calculated using the mathematical formula

$$Q = 2\pi \int_{r=0}^{r=h} w(r, t) r dr \tag{39}$$

Using equation (39) to calculate the flow rate, we have:

$$Q = 2\pi e^{i\omega t} \int_{r=0}^{r=h} \left( B_3 r I_0(\beta_1 r) + A_4 r + A_6 r I_0(\beta_4 r) + A_7 r^3 + A_8 r^5 \right) dr \tag{40}$$

Simplifying equation (40), we have:

$$Q = 2\pi e^{i\omega t} \left( B_3 h I_1(\beta_1 h) + A_6 h I_1(\beta_4 h) + \frac{A_4 h^2}{2} + \frac{A_7 h^4}{4} + \frac{A_8 h^6}{6} \right) \tag{41}$$

#### 4. Results

Here, we investigate the influence of the various parameters on the blood velocity profile and concentration profile as shown in Figs 1-8. For the numerical simulation, the values of the suggested parameters are within the range such as  $0 \leq Sr \leq 10, 0 \leq Gc \leq 25, 0 \leq Pr \leq 10, 0 \leq M \leq 10, 0 \leq Sc \leq 1, 0 \leq \omega \leq 2$  at the location in the arterial channel  $x = 0.5$ .

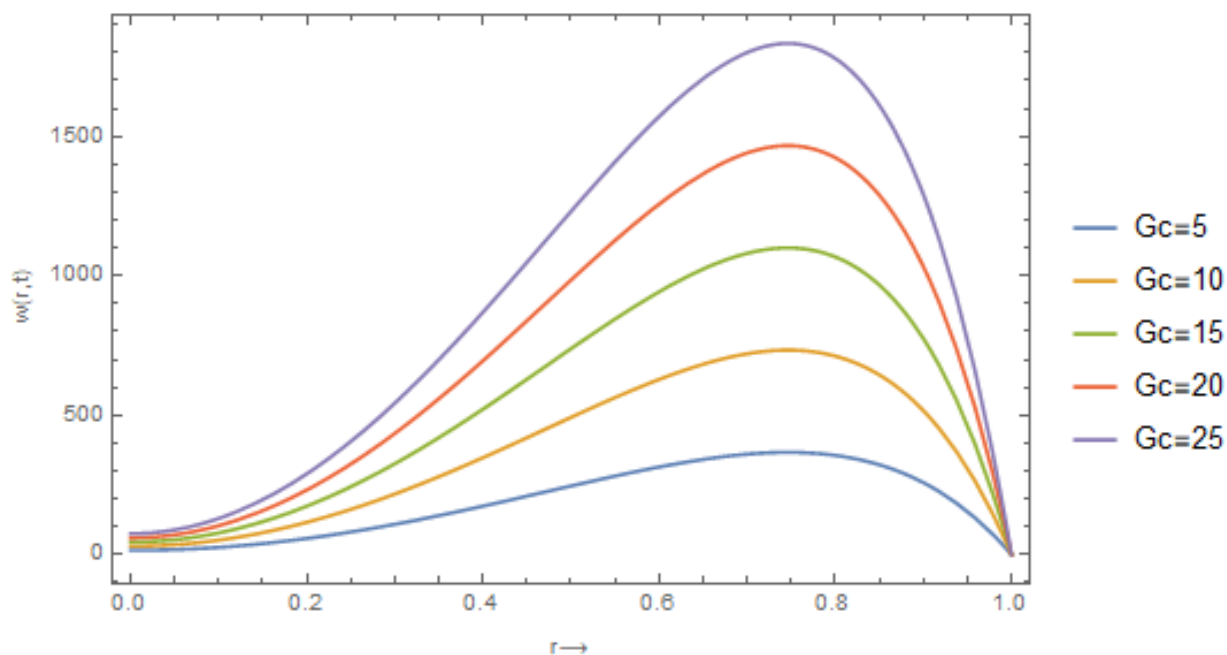


Figure 2. Influence of Solutal Grashof number on Blood Velocity with other values  $Sr = 2, Pr = 2.1, Sc = 0.2, Rd_3 = 2, Rd_1 = 2, \omega = 0.3, k = 0.05, M = 1.5, x = 0.5$

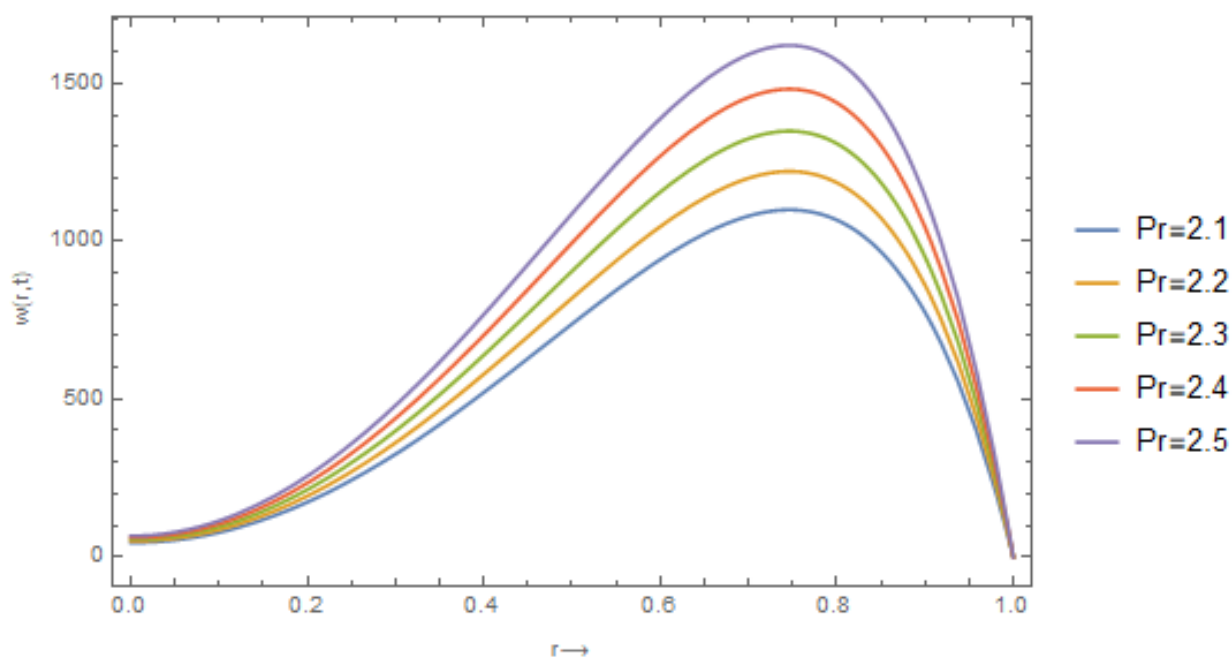


Figure 3. Influence of Prandtl number parameter on Blood Velocity with other values as  $Sr = 2, Gc = 15, Sc = 0.2, Rd_3 = 2, Rd_1 = 2, \omega = 0.3, k = 0.05, M = 1.5, x = 0.5$

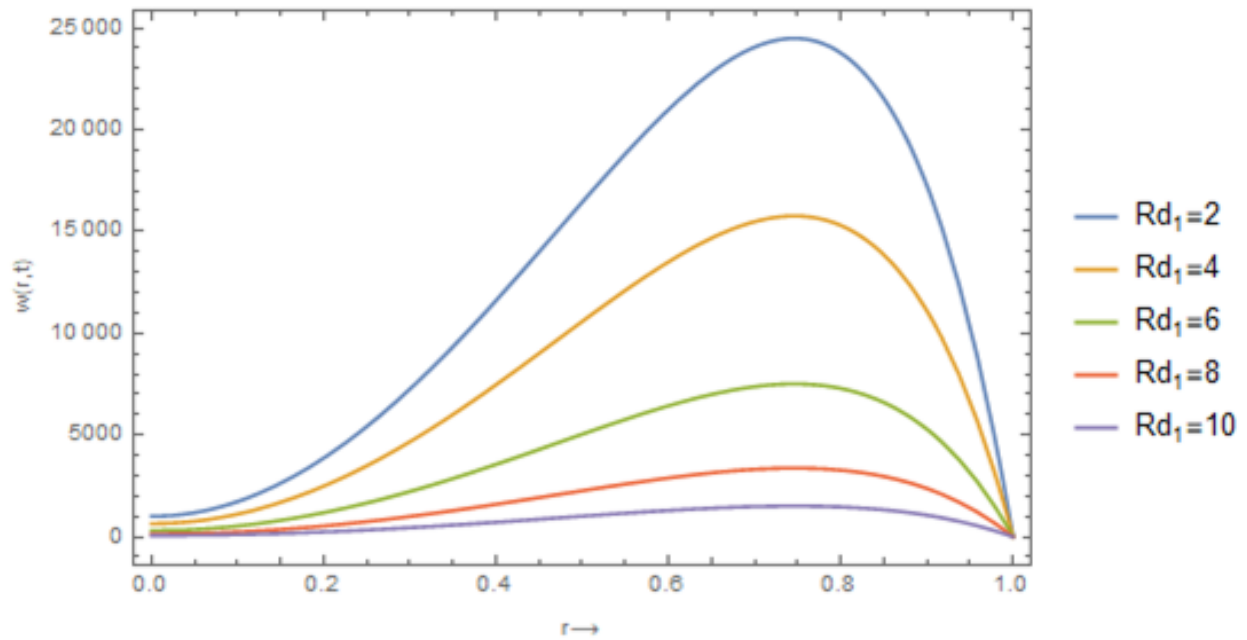


Figure 4. Influence of Radiation parameter on Blood Velocity with other values as  $Sr = 2, Gc = 15, Pr = 2.1, Sc = 0.2, Rd_3 = 2, \omega = 0.3, k = 0.05, M = 1.5, x = 0.5$

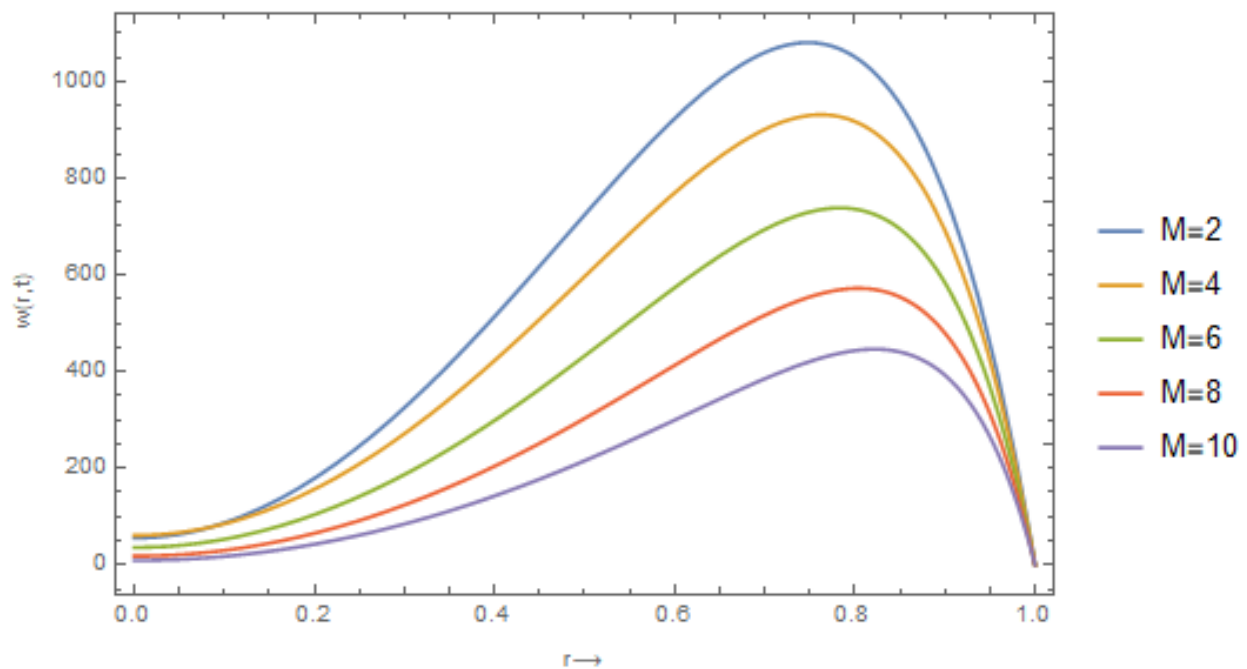


Figure 5. Influence of Magnetic Field on Blood Velocity with other values as  $Sr = 2, Gc = 15, Pr = 2.1, Sc = 0.2, Rd_3 = 2, Rd_1 = 2, \omega = 0.3, k = 0.05, x = 0.5$

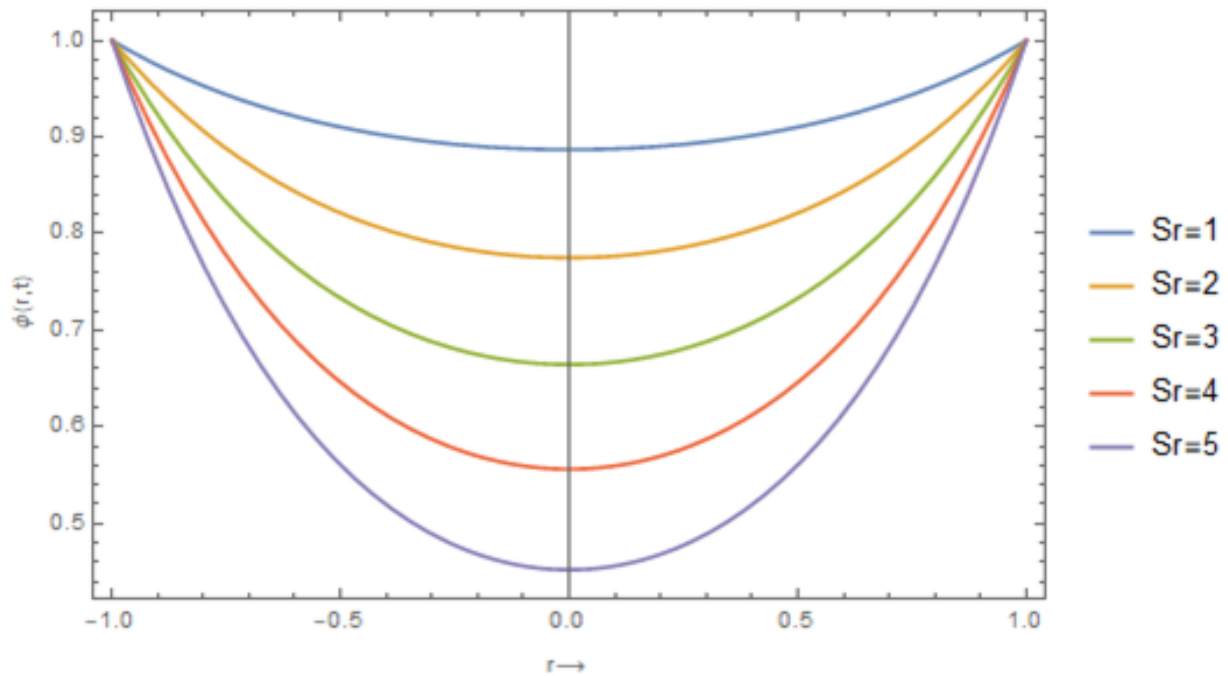


Figure 6. Influence of Soret number parameter on concentration with other values as  $Pr = 2.1, Sc = 0.2, Rd_1 = 2, \omega = 0.3, x = 0.5$   $Pr = 2.1, Sc = 0.2, Rd_1 = 2, \omega = 0.3, x = 0.5$

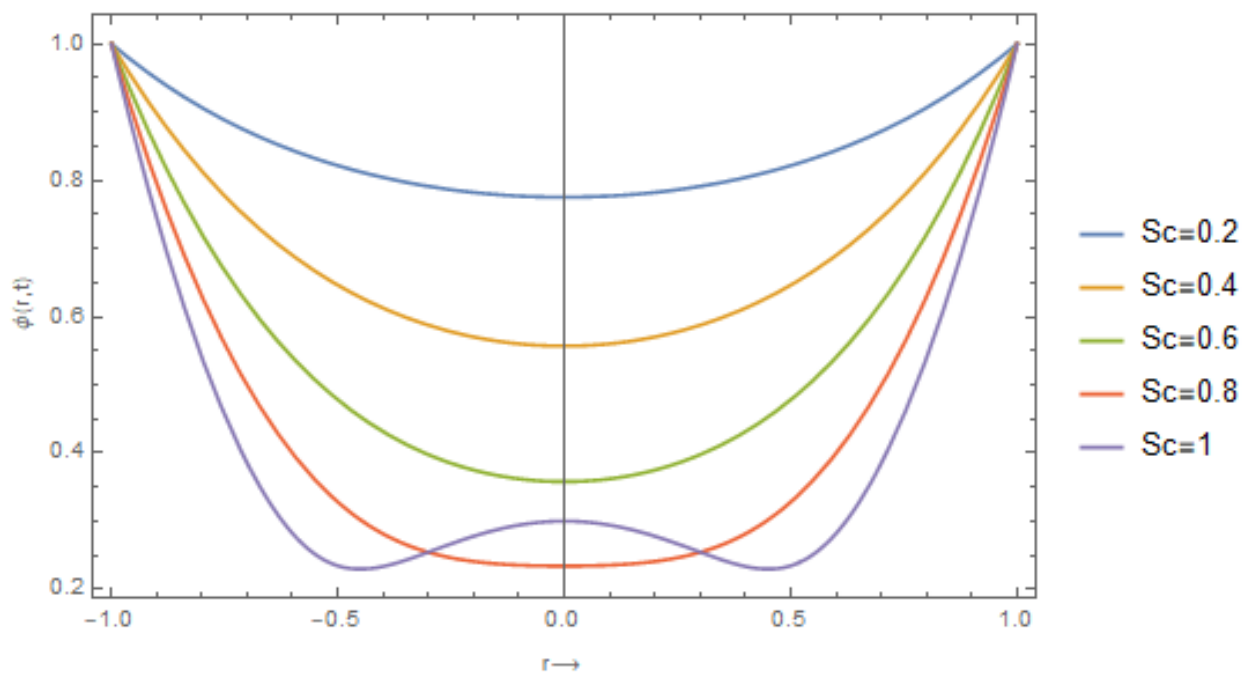


Figure 7. Influence of Schmidt number parameter on concentration with other values as  $Pr = 2.1, \omega = 0.3, Rd_1 = 2, Sr = 2, x = 0.5$   $Pr = 2.1, \omega = 0.3, Rd_1 = 2, Sr = 2, x = 0.5$

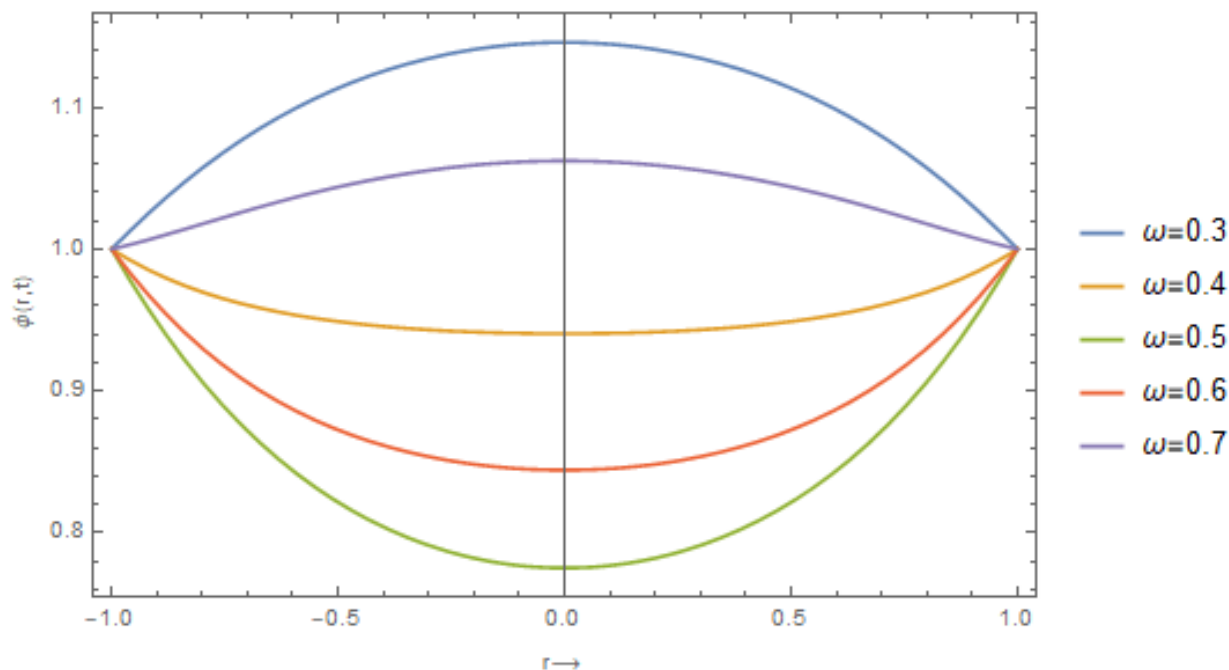


Figure 8. Influence of Oscillatory frequency parameter on concentration with other values as  $Pr = 2.1, Sc = 0.2, Rd_1 = 2, Sr = 2, x = 0.5$   
 $Pr = 2.1, Sc = 0.2, Rd_1 = 2, Sr = 2, x = 0.5$

## 5. Discussion

Figure 1 illustrates the influence of Soret number  $Sr = 1, 2, 3, 4, 5$  on the blood velocity at the location  $x = 0.5$ . It is observed that the velocity increases for each value of the Soret number, as depicted. Figure 2 shows the influence of solutal Grashof number,  $Gc = 5, 10, 15, 20, 25$  on blood velocity passing through the segment  $x = 0.5$ . It was observed that the velocity increases for each value of the Grashof number, as seen. The influence of Prandtl number was investigated and the simulation is shown in Figure 3. The figure shows the influence of Prandtl number  $Pr = 2.1, 2.2, 2.3, 2.4, 2.5$  on blood velocity as it passes through the location. It is seen that an increase in Prandtl number causes the blood velocity to decrease. Figure 4 explains the influence of the radiation parameter value  $Rd_1 = 2, 4, 6, 8, 10$  on blood velocity passing through the location  $x = 0.5$ . It was observed that radiation increased caused the blood velocity to increase for different radiation parameter values, which agrees with Bunonyo and Eli [20]. Figure 5 explains the influence of the magnetic field parameter value  $M = 2, 4, 6, 8, 10$  on blood velocity through the location  $x = 0.5$ . We noticed that the blood velocity decreases for every increase in a magnetic field. The application of applied magnetic field plays a vital role in the study of blood flow because it can be used as a treatment for heart-related diseases. This result agrees with previous research by Hanvey and Bunonyo [17], as well as Bunonyo and Ebiwareme [19]. The study investigated the influence of Soret number on cholesterol concentration with the result shown in Figure 6; the figure is of the view that the concentration decreases with the increase in different values of the Soret number  $Sr = 1, 2, 3, 4, 5$  at the location at  $x = 0.5$ . Figure 7 illustrates the influence of the Schmidt number  $Sc = 0.2, 0.4, 0.6, 0.8, 1.0$  on cholesterol concentration in the fluid flow passing through a particular location  $x = 0.5$ . It explains that the concentration decreases for every increase in Schmidt number, and this result agrees with Misra and Adhikary [21]. Figure 8 depicts the influence of the oscillatory frequency  $\omega = 0.3, 0.4, 0.5, 0.6, 0.7$  on cholesterol concentration in the fluid passing through the location. It was observed that the concentration decreased for various values of the oscillatory frequency.

## 6. Conclusion

In this study, we have investigated the convective flow of blood through a constricted cylinder and the effect of cholesterol growth rate on the motion in the presence of a magnetic field. On solving the governing mathematical models and performing numerical simulation using Wolfram Mathematica, the results are presented graphically. Furthermore, the results have been discussed. We can conclude as follows:

- The blood velocity increased for an increase in sorbitol to a maximum level before it decreased to zero when the sclerotic level was high.
- The study revealed that the blood velocity decreased for an increase in solutal Grashof number and it reached a peak before decreasing to a minimum value.
- It was revealed that the blood velocity decreases for an increase in Schmidt number, and it grew to a maximum and converged to zero along the channel.
- The Prandtl number decreases the blood velocity as revealed in the result. However, the velocity increases due to an increase in radiation parameter value.
- The magnetic field increase causes a decrease in blood velocity due to the Lorentz force generated.
- An increase in Soret number causes a decrease in cholesterol concentration in the fluid, and it converges when the boundary layer is at its peak.
- The concentration decreases for every increase in Schmidt numbers along the channel.
- An increase in oscillatory frequency causes a corresponding increase in concentration.

This research could be extended by considering the flow in an inclined channel and could be solved using a series method with time independency.

## Acknowledgements

The authors are very grateful to the anonymous reviewers for their careful reading of this manuscript and helpful suggestions in the form of contributions.

## References

- [1] K.W. Bunonyo, E. Amos & J.B. Goldie, “Mathematical Modelling of an Atherosclerotic Blood Flow Through Double Stenosed Region with Application of Treatment”, *International Journal of Applied Mathematics and Theoretical Physics* **6** (2020) 19.
- [2] D. Ambrosi, & F. Mollica, “On the mechanics of a growing tumor”, *International journal of engineering science* **40** (2002) 1297. [https://doi.org/10.1016/S0020-7225\(02\)00014-9](https://doi.org/10.1016/S0020-7225(02)00014-9)
- [3] D. Balzani & T. Schmidt, “Comparative analysis of damage functions for soft tissues: Properties at damage initialization. *Mathematics and mechanics of solids*”, **20** (2015) 480.
- [4] G. R. Barrenechea & F. Valentin, “An unusual stabilized finite element method for a generalized Stokes problem”, *Numerische Mathematik* **92** (2002) 653.
- [5] Y. Bazilevs, J. R. Gohean, T. J. Hughes, R. D. Moser & Y. Zhang, “Patient-specific isogeometric fluid–structure interaction analysis of thoracic aortic blood flow due to implantation of the Jarvik 2000 left ventricular assist device”, *Computer Methods in Applied Mechanics and Engineering* **198** (2009) 3534. <https://doi.org/10.1016/j.cma.2009.04.015>
- [6] A. J. Brown, Z. Teng, P. C. Evans, J. H. Gillard, H. Samady & M. R. Bennett, “Role of biomechanical forces in the natural history of coronary atherosclerosis”, *Nature reviews cardiology* **13** (2016) 210.
- [7] V. Calvez, J. G. Houot, N. Meunier, A. Raoult & G. Rusnakova. “Mathematical and numerical modeling of early atherosclerotic lesions”, In *ESAIM: Proceedings* **30** (2010) 1. <https://doi.org/10.1051/proc/2010002>
- [8] A. D. Chalmers, A. Cohen, C. A. Bursill & M. R. Myerscough, “Bifurcation and dynamics in a mathematical model of early atherosclerosis”, *Journal of mathematical biology* **71** (2015) 1451.

- [9] J. Chen & X. Y. Lu, “Numerical investigation of the non-Newtonian pulsatile blood flow in a bifurcation model with a non-planar branch”, *Journal of biomechanics* **39** (2006) 818. <https://doi.org/10.1016/j.jbiomech.2005.02.003>
- [10] C. Cheng, F. Helderma, D. Tempel, D. Segers, B. Hierck, R. Poelmann, A. Van Tol, D. J. Duncker, D. Robbers-Visser, N. T. Ursem & R. Van Haperen, “Large variations in absolute wall shear stress levels within one species and between species”, *Atherosclerosis* **195** (2007) 225. <https://doi.org/10.1016/j.atherosclerosis.2006.11.019>
- [11] Y. I. Cho & K. R. Kenney, “Effects of the non-Newtonian viscosity of blood on flows in a diseased arterial vessel”, Part 1: Steady flows. *Biorheology* **28** (1991) 241.
- [12] M. Cilla, E. Pena & M. A. Martinez, “Mathematical modelling of atheroma plaque formation and development in coronary arteries”, *Journal of The Royal Society Interface* **11** (2014) 20130866 <https://doi.org/10.1098/rsif.2013.0866>
- [13] R. Codina, “Stabilized finite element approximation of transient incompressible flows using orthogonal subscales”, *Computer methods in applied mechanics and engineering* **191** (2002) 4295. [https://doi.org/10.1016/S0045-7825\(02\)00337-7](https://doi.org/10.1016/S0045-7825(02)00337-7)
- [14] P. Crosetto, P. Reymond, S. Deparis, D. Kontaxakis, N. Stergiopoulos & A. Quarteroni, “Fluid–structure interaction simulation of aortic blood flow”, *Computers & Fluids* **43** (2011) 46. <https://doi.org/10.1016/j.compfluid.2010.11.032>
- [15] D. De Wilde, B. Trachet, G. De Meyer & P. Segers, “The influence of anesthesia and fluid–structure interaction on simulated shear stress patterns in the carotid bifurcation of mice”, *Journal of biomechanics* **49** (2016) 2741. <https://doi.org/10.1016/j.jbiomech.2016.06.010>
- [16] J. Moradicheghamahi, J. Sadeghiseraji & M. Jahangiri, “Numerical solution of the Pulsatile, non-Newtonian and turbulent blood flow in a patient specific elastic carotid artery”, *International Journal of Mechanical Sciences* **150** (2019) 393. <https://doi.org/10.1016/j.ijmecsci.2018.10.046>
- [17] R. R. Hanvey & K. W. Bunonyo, “Effect of Treatment Parameter on Oscillatory Flow of Blood Through an Atherosclerotic Artery with Heat Transfer”, *Journal of the Nigerian Society of Physical Sciences* **4** (2022) 682. <https://doi.org/10.46481/jnsps.2022.682>
- [18] B. W. Kubugha & E. Amos, “Mathematical Modeling of LDL-C and Blood Flow through an Inclined Channel with Heat in the Presence of Magnetic Field”, *Trends in Sciences* **19** (2022) 5693. <https://doi.org/10.48048/tis.2022.5693>
- [19] K. W. Bunonyo & L. Ebiwareme, “A Low Prandtl Number Haemodynamic Oscillatory Flow through a Cylindrical Channel using the Power Series Method”, *European Journal of Applied Physics* **4** (2022) 56.
- [20] J. C. Misra & S. D. Adhikary, “MHD oscillatory channel flow, heat and mass transfer in a physiological fluid in presence of chemical reaction”, *Alexandria Engineering Journal* **55** (2016) 287. <https://doi.org/10.1016/j.aej.2015.10.005>
- [21] K. W. Bunonyo & G. D. Eli, “Convective Fluid Flow through a Sclerotic Oscillatory Artery in the Presence of Radiative Heat and a Magnetic Field”, *Asian Journal of Pure and Applied Mathematics* **4** (2022) 258.

## Nomenclature

- $x^*$  Dimensional coordinate along the channel  
 $r^*$  Dimensional coordinate perpendicular to the channel  
 $R$  Radius of an abnormal channel  
 $R_0$  Radius of normal channel  
 $P_0$  Systolic pressure  
 $Rd_1$  Radiation parameter  
 $Rd_3$  Chemical reaction parameter  
 $k_{Tb}$  Blood thermal conductivity  
 $w^*$  Dimensional velocity profile  
 $w$  Dimensionless velocity profile  
 $w_0$  Perturbed velocity profile  
 $C^*$  Dimensional lipid particle concentration  
 $C_\infty$  Far field cholesterol particle concentration  
 $c_{bp}$  The specific heat capacity of blood  
 $t^*$  Dimensionless time  
 $T$  Temperature of the fluid  
 $T_\infty^*$  Far field temperature  
 $T_w^*$  Temperature at the wall  
 $B_0$  Magnetic field  
 $M$  Magnetic field parameter  
 $a$  Growth rate of LDL-cholesterol

## Greek Symbols

- $\nu_b$  Kinematic viscosity of blood

- $\mu_b$  Dynamic viscosity of blood
- $Pr$  Prandtl number for blood
- $g$  Acceleration due to gravity
- $\delta^*$  Dimensional height of stenosis
- $\sigma_e$  Electrical conductivity
- $\lambda^*$  Length of stenosis
- $\omega$  Oscillatory frequency
- $\theta$  Dimensionless blood temperature
- $\phi$  Dimensionless cholesterol particle concentration
- $\theta_a$  Dimensionless wall temperature
- $\theta_0$  Perturbed blood temperature profile
- $\phi_a$  Dimensionless wall lipid concentration
- $\phi_0$  Perturbed lipid concentration
- $\rho_b$  Blood density

**Subscripts**

- $w$  Wall
- $b$  Blood
- $e$  Electrical
- $T$  Thermal
- $\infty$  Far field
- MMDARG Mathematical Modelling and Data Analytics Research Group

**Appendix**

$$\beta_1^2 = \left( \frac{1}{k} + M^2 + i\omega \right), \beta_2^2 = (Rd_1 + i\omega) Pr, \beta_3^2 = (Rd_3 + i\omega) Sc, \beta_4^2 = Sc i\omega$$

$$J_0(i\beta_1 r) = I_0(\beta_1 r)$$

$$\beta_1^2 = \left( \frac{1}{k} + M^2 + i\omega \right), \beta_2^2 = (Rd_1 + i\omega) Pr, \beta_4^2 = Sc i\omega$$

$$A_1 = \frac{S_r S c e^{-i\omega t}}{\beta_4^2 I_0(\beta_2 h)} \left( \beta_2^2 + \left( \frac{\beta_2^4}{\beta_3^2} + \frac{\beta_2^6}{\beta_4^4} \right) \right), A_2 = \frac{S_r S c e^{-i\omega t}}{4 I_0(\beta_2 h)} \left( \frac{\beta_2^4}{\beta_3^2} + \frac{\beta_2^6}{\beta_4^4} \right), A_3 = \frac{S_r S c e^{-i\omega t}}{64 I_0(\beta_2 h)} \frac{\beta_2^6}{\beta_4^4}$$

$$A_4 = -\frac{P_0}{\beta_1^2} + \frac{A_1 G c}{\beta_1^2} + 4 \left( \frac{A_2 G c}{\beta_1^4} + \frac{16 A_3 G c}{\beta_1^6} \right), A_6 = \frac{A_0 G c}{\beta_1^2}, A_7 = \frac{A_2 G c}{\beta_1^2} + \frac{16 A_3 G c}{\beta_1^4}, A_8 = \frac{A_3 G c}{\beta_1^2}$$

$$B_3 = -\frac{A_4}{I_0(\beta_1 h)} - A_6 \frac{I_0(\beta_4 h)}{I_0(\beta_1 h)} - \frac{A_7 h^2}{I_0(\beta_1 h)} - \frac{A_8 h^4}{I_0(\beta_1 h)}, A_0 = \frac{e^{-i\omega t}}{I_0(\beta_4 h)} - \frac{A_1}{I_0(\beta_4 h)} - \frac{A_2 h^2}{I_0(\beta_4 h)} - \frac{A_3 h^4}{I_0(\beta_4 h)}$$

$$\int r I_0(r) dr = r I_1(r),$$

$$I_0(\beta_2 r) = \left( 1 + \frac{\beta_2^2 r^2}{4} + \frac{\beta_2^4 r^4}{64} + \frac{\beta_2^6 r^6}{2304} + \dots \right), \text{ and } I_1(\beta_2 r) = \left( \frac{2\beta_2^2 r}{4} + \frac{4\beta_2^4 r^3}{64} + \frac{6\beta_2^6 r^5}{2304} + \dots \right)$$

$$I_1'(\beta_2 r) = \left( \frac{2\beta_2^2}{4} + \frac{12\beta_2^4 r^2}{64} + \frac{30\beta_2^6 r^4}{2304} + \dots \right) \text{ and } I_0(\beta_2 h) = \left( 1 + \frac{\beta_2^2 h^2}{4} + \frac{\beta_2^4 h^4}{64} + \frac{\beta_2^6 h^6}{2304} + \dots \right)$$